

Decentralized PI Controller with Coefficient Diagram Method Incorporating Feedforward Controller Based on Inverted Decoupling for Two Input – Two Output System

Abstract. A decentralized PI controller for a TITO system of Wood-Berry distillation column process combined with inverted decoupling is designed by using the coefficient diagram method (CDM) with feedforward controller (FFC). The ability of CDM and CDM with FFC methods to design controllers for the desired transient response has been investigated for TITO system. By using the CDM adding FFC, a good and competitive performance can be achieved with faster settling time that the slight percent overshoot is neglected although an increasing control signal is provided.

Streszczenie. Przedstawiono sterowanie procesem destylacji w systemie dwa wejścia-dwa wyjścia przy wykorzystaniu metody Coefficient Diagram ze sterownikiem typu feedforward. Osiągnięto skrócenie czasu ustalania przy małym przeregulowaniu. Sterowanie procesem destylacji przy wykorzystaniu metody Coefficient Diagram i dla systemu dwa wejścia – dwa wyjścia.

Keywords: Coefficient Diagram Method, Decentralized controller, Feedforward controller, Inverted decoupling, TITO system

Słowa kluczowe: metoda Coefficient Diagram, system dwa wejścia-dwa wyjścia.

Introduction

Most industrial processes have multiple-input multiple-output (MIMO) structure which provides the complex control system because the most significant character with the MIMO systems is cross interactions among the variables [1]. Because of the multivariable processes and the loop interactions, the controller design and tuning of multi-loop give more difficult as compared to that of single loop controllers. The controller design techniques for interactive MIMO systems are generally classified as centralized or decentralized controllers [1, 2] when for many decades, the decentralized controller for multi-loop system has been predominantly applied because this type of controller is simple to design and easy to tune, implement and maintain [3, 4].

Decentralized control design with decoupling technique is most commonly applied for MIMO systems. Decoupling, which is one of the advanced regulatory control strategies, is designed to transform the multivariable process to a diagonal dominant plant, allowing individual design of a controller for each loop [5]. Two-input two-output (TITO) systems are one of the most extensive categories of multivariable processes in industries [6]. For the controller design of TITO systems, the decoupler matrix method is used to decompose a multi-loop control system into a set of equivalent independent single loops [7]. So far, there are many studies on decoupling techniques, especially the control design of TITO processes in which the advantages and limitations of each decoupling technique were investigated [8-10]. Among the various types of decoupling techniques, an inverted decoupling technique is one of the most major types of dynamic decoupling techniques [11]; even though it is rarely implemented, it combines main advantage of both the simplified and ideal decoupling methods [8]. Based on the inverted decoupling technique, the controllers of many TITO processes have been designed by using various methodologies such as an active disturbance rejection control for multi-variable systems [5], internal model control [11-13], Multiple-integration (MI) technique and Magnitude-optimum (MO) tuning method [14], Smith predictor [15], and the convexification strategy of the Generalized Geometric Programming (GGP) method [16].

Moreover, in our previous work [17-18], the inverted decoupling technique for the TITO system of the well-known Wood-Berry distillation column process [19], which is one

of the most noticeable case studies to investigate various methods of controller design, has been carried out. A decentralized PID controller based on inverted decoupling was designed by using the root locus method [17] providing good performance to maintain the controlled variables and giving smoother output and control signal responses than that introduced by Maghade and Patre [4] and, in addition, the settling time and control signal can be competitive with the performance of controller design introduced by Tavakoli et al. [6] although the percent overshoot of this proposed method is higher than that of Tavakoli's control design. However, by using the coefficient diagram method (CDM) instead of the root locus, the decentralized PID controller design for Wood-Berry distillation column combined with inverted decoupling also gave effectiveness in controlling the process variables without the percent overshoot of responses of control variables [18]. This is because the key features of CDM, when the numerator and denominator of the transfer function are considered independently from each other, are alteration of the polynomial approaches for the plant and the controller, nonexistence or existence of very small overshoot in the closed loop response, obtaining the characteristic polynomial of the closed loop system efficiently by taking a good balance of stability [20]. Additionally, the main advantage of CDM is its simplicity and good robust controller for several industrial processes under practical limitation and many control systems have been effectively applied by using CDM. Nevertheless, the research concerning the control design based on the inverted decoupling technique by using CDM for the Wood-Berry process combined with inverted decoupling is limited [18]. Because of tuning of various control parameters of PID controllers, the use of PI controllers provides many practical advantages such as their simple control structure, fewer tuning parameters, robustness against sensor/actuator failure, and easy understandability [21]. The methods for decentralized PI controllers with decoupler have been designed by using the gain and phase margin specifications [4], the minimum integral absolute error (IAE) [21], the auto-tuning [22], and the non-dimensional tuning [23].

In this study, the decentralized PI controller design using CDM based on inverted decoupling for the Wood-Berry distillation column process is investigated. However, according to a design of CDM, the PI controller parameters are obtained based on the stability and the speed of the controlled system, designed from the stability index and the

equivalent time constant at a specified settling time, respectively, that is, CDM can only be obtained by specifying the stability index [24-26]. Owing to an increase of the stability index value resulting in longer settling time [27-28], to improve faster settling time in the transient response period of control system, this multivariable control system is considered to add a feedforward controller (FFC) into the decentralized PI controllers with inverted decoupling. The PI controllers with FFC designed by CDM have been continuously performed for single-input single-output (SISO) systems such as level process [24], temperature control system [25] and flow control system [26]. An additional controller of I-PDA of AC induction motor designed by using CDM with FFC was also proposed [29]. However, the studies relating to the decentralized PI controller design using CDM based on inverted decoupling with FFC for TITO process are limited. As mentioned above, this paper focuses on the comparison of the decentralized PI controller using CDM and CDM with FFC based on inverted decoupling for the TITO process of Wood-Berry distillation column.

Concept of Coefficient Diagram Method

Fig. 1 illustrates the standard block diagram of the CDM control system where $B_p(s)$ and $A_p(s)$ are numerator and denominator in terms of the polynomial transfer functions of the plant. $A_c(s)$ is the forward denominator polynomial; $B_f(s)$ and $B_c(s)$ are considered as the reference numerator and the feedback numerator polynomials in CDM controller transfer functions, respectively. Since the controller transfer function has two numerators, it is similar to 2-DOF (two-degree of freedom) control system structure. $A_c(s)$ and $B_c(s)$ are designed by giving a required transient behaviour, whereas $B_f(s)$, called as pre-filter and used for set-point tracking, is calculated to provide the steady-state gain for obtaining the response with zero steady-state error. The output of the CDM control system from Fig. 1 can be written as

$$(1) \quad Y(s) = \frac{B_p(s)B_f(s)}{P(s)}R(s) + \frac{A_p(s)A_c(s)}{P(s)}D(s)$$

where $P(s)$ is the characteristic polynomial of the close loop system as defined by

$$(2) \quad P(s) = A_c(s)A_p(s) + B_c(s)B_p(s) \\ = a_n s^n + a_{n-1} s^{n-1} + \dots + a_1 s + a_0 = \sum_{i=0}^n a_i s^i$$

where a_0, a_1, \dots, a_n are the real coefficients.

According to Manabe [30], the CDM parameters consisting of equivalent time constant (τ), stability index (γ_i) and stability limits (γ_i^*) can be determined by Eqs. (3), (4) and (5), respectively [31].

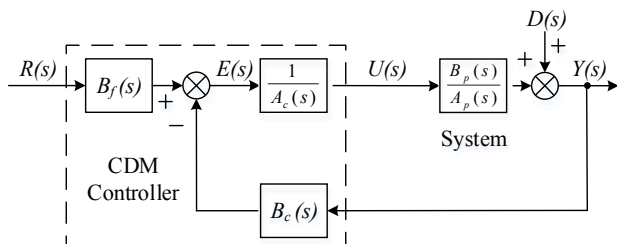


Fig. 1. Standard block diagram of CDM control system

$$(3) \quad \tau = \frac{a_1}{a_0}$$

$$(4) \quad \gamma_i = \frac{a_i^2}{(a_{i-1}a_{i+1})}; \quad i = 1, \dots, n-1$$

$$(5) \quad \gamma_i^* = \frac{1}{\gamma_{i+1}} + \frac{1}{\gamma_{i-1}}; \quad \gamma_o = \gamma_n = \infty$$

The main designed parameters of CDM are the equivalent time constant and the stability index. Firstly, the equivalent time constant is calculated at the desired settling time for the time response of the CDM control system. The relation between the settling time and the equivalent time constant is adjusted consistent with the standard Manabe form [30]. If t_s denotes the desired settling time, the relation express of the chosen τ can be given by

$$(6) \quad \tau = \frac{t_s}{(2.5 \sim 3)}$$

As introduced by the Manabe form [30], the stability index is selected as

$$(7) \quad \gamma_1 = 2.5; \quad \gamma_i = 2, \quad i = 2 \sim (n-1); \quad \gamma_o = \gamma_n = \infty$$

The standard values of stability index as stated in Manabe form [30] can be utilized to design the controller if the following condition as presented in Eq. (8) is satisfied.

$$(8) \quad p_k / p_{k-1} > \tau / (\gamma_{n-1} \gamma_{n-2} \dots \gamma_1)$$

where p_k and p_{k-1} are the coefficients of the plant at k^{th} and $(k-1)^{\text{th}}$ order, respectively. If the above condition is not satisfied, γ_{n-1} can be first increased then γ_{n-2} and so on, until Eq. (8) is satisfied. When the designed parameters τ and γ_i are specified, a target characteristic polynomial, $P_{\text{target}}(s)$ is determined by

$$(9) \quad P_{\text{target}}(s) = a_0 \left[\sum_{i=2}^n \left(\prod_{j=1}^{i-1} \frac{1}{\gamma_{i-j}} \right) (\tau s)^i + \tau s + 1 \right]$$

By equating the two characteristic polynomials in Eq. (2) and Eq. (9), a Diophantine equation is attained as Eq. (10). Then, the controller parameters are certainly achieved by solving this equation.

$$(10) \quad P_{\text{target}}(s) = A_c(s)A_p(s) + B_c(s)B_p(s)$$

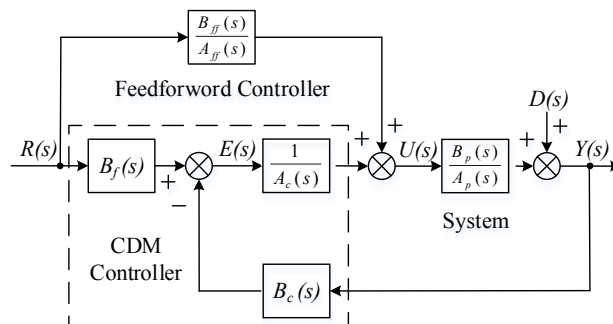


Fig. 2. Standard block diagram of CDM control system with FFC

Coefficient Diagram Method with Feedforward Controller

To reduce the long settling time caused by the large value of the stability index from CDM designed for PI controller, a feedforward controller (FFC) is added in the decentralized PI controller system based on inverted decoupling which is designed by using CDM as shown in Fig. 2 where $B_{ff}(s)$ and $A_{ff}(s)$ are numerator and

denominator as the polynomial transfer functions of the FFC. The standard block diagram of CDM with FFC can be rearranged in a structure of 2-DOF with FFC as shown in Fig. 3 at which the system $G_p(s)$, the feedback controller $G_c(s)$, the forward controller $G_f(s)$ and the feedforward controller $G_{ff}(s)$ are defined as in Eqs. (11) - (14), respectively.

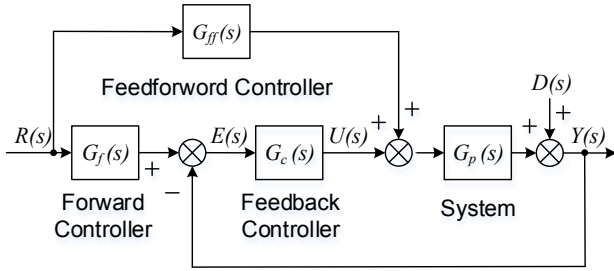


Fig.3. Two-Degree of Freedom Control system with FFC

$$(11) \quad G_p(s) = \frac{B_p(s)}{A_p(s)}$$

$$(12) \quad G_c(s) = \frac{B_c(s)}{A_c(s)}$$

$$(13) \quad G_f(s) = \frac{B_f(s)}{B_c(s)}$$

$$(14) \quad G_{ff}(s) = \frac{B_{ff}(s)}{A_{ff}(s)}$$

The transfer function of the CDM control system with FFC in Fig. 3 can be obtained as

$$(15) \quad \frac{Y(s)}{R(s)} = \frac{G_p(s)[G_{ff}(s) + G_c(s)G_f(s)]}{[1 + G_p(s)G_c(s)]} = \frac{B_p(s)F(s)}{A_{ff}(s)P(s)}$$

where $F(s)$ the polynomial function caused by an added feedforward controller as defined by

$$(16) \quad F(s) = B_f(s)A_{ff}(s) + B_{ff}(s)A_c(s)$$

An effect of the feedforward controller on transfer function in Eq. (15) can be used to decrease transient response time of the control system. However, $F(s)$ in Eq. (15) has no effect on the output transfer function concerning disturbance. Therefore, the desired transfer function used for controller design is as follows

$$(17) \quad \frac{F(s)}{P(s)} = \frac{B(s)}{A(s)} = \frac{B_f(s)A_{ff}(s) + B_{ff}(s)A_c(s)}{A_c(s)A_p(s) + B_c(s)B_p(s)}$$

Rearranging Eq. (17) into polynomial form gives

$$(18) \quad \frac{B(s)}{A(s)} = \frac{b_m s^m + b_{m-1} s^{m-1} + \dots + b_1 s + b_0}{a_n s^n + a_{n-1} s^{n-1} + \dots + a_1 s + a_0}$$

where a_0, a_1, \dots, a_n are the constant coefficients of $A(s)$ and b_0, b_1, \dots, b_m are the constant coefficients of $B(s)$ when $m \leq n$.

As presented in Eq. (18), the denominator polynomial $A(s)$ is the characteristic polynomial of the considered control system that the constant coefficients can be determined by

$$(19) \quad A(s) = a_0 \left[\sum_{i=2}^n \left(\prod_{j=1}^{i-1} \frac{1}{\gamma_{i-j}} \right) (\tau s)^i \right] + \tau s + 1$$

The constant coefficients of the numerator polynomial $B(s)$ can be obtained and used to design the controller parameters of the closed-loop system by using CDM [27, 32]. Thus, the coefficients of the numerator polynomial (b_i) can be given by

$$(20) \quad b_i = \frac{b_0 (\nu \tau)^i}{\gamma_{i-1} \dots \gamma_2^{i-2} \gamma_1^{i-1}} = b_0 (\nu \tau)^i \prod_{i=1}^{i-1} \frac{1}{(\gamma_{i-j})^j}$$

where ν is the tuning factor at $0 < \nu < 1$. The equivalent time constant τ is scaled by tuning factor (ν); consequently the response speed can be adjusted. Substituting each coefficient into the numerator polynomial $B(s)$ yields

$$(21) \quad B(s) = b_0 \left[\sum_{i=2}^n \left(\prod_{j=1}^{i-1} \frac{1}{\gamma_{i-j}} \right) (\nu \tau s)^i \right] + \nu \tau s + 1$$

Substituting Eqs. (19) and (21) into Eq. (18) results in the transfer function in terms of τ , γ_i , and ν according to CDM as follows

$$(22) \quad \frac{B(s)}{A(s)} = \frac{b_0 \left[\sum_{i=2}^n \left(\prod_{j=1}^{i-1} \frac{1}{\gamma_{i-j}} \right) (\nu \tau s)^i \right] + \nu \tau s + 1}{a_0 \left[\sum_{i=2}^n \left(\prod_{j=1}^{i-1} \frac{1}{\gamma_{i-j}} \right) (\tau s)^i \right] + \tau s + 1}$$

As presented in Eq. (22), the 2-DOF control system with FFC using CDM is performed to achieve a design of controller parameters based on the stability and the speed of the controlled system. By using CDM the stability is designed from the suitable stability index γ_i , and the speed depends on the equivalent time constant τ calculated from t_s . When FFC is added into the control system, the speed can be additionally adjusted by using the tuning factor ν .

System Structure and Controller Design

The structure of TITO feedback control system with an inverted decoupling is demonstrated in Fig. 4 that the transfer function matrix of TITO process is given by

$$(23) \quad G(s) = \begin{bmatrix} G_{11}(s) & G_{12}(s) \\ G_{21}(s) & G_{22}(s) \end{bmatrix}$$

The transfer function matrix of inverted decoupler [12] is

$$(24) \quad D(s) = \begin{bmatrix} D_{11}(s) & D_{12}(s) \\ D_{21}(s) & D_{22}(s) \end{bmatrix}$$

Inverted decouplers are included into TITO process to eliminate the loop interactions to be SISO process that

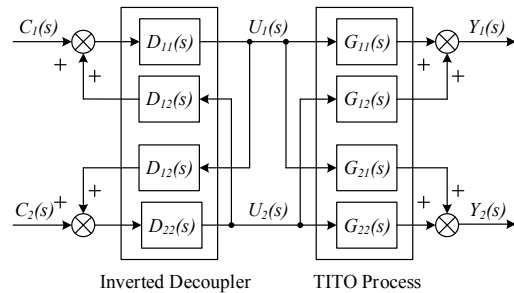


Fig.4. Inverted decoupling of TITO process

a product of transfer function of $G(s)D(s)$ is a diagonal transfer matrix $T(s)$ as follows

$$(25) \quad T(s) = G(s)D(s) = \begin{bmatrix} G_{11}(s) & 0 \\ 0 & G_{22}(s) \end{bmatrix}$$

Rearranging Eqs. (24) and (25) yields [33]

$$(26) \quad \begin{bmatrix} D_{11}(s) & D_{12}(s) \\ D_{21}(s) & D_{22}(s) \end{bmatrix} = \begin{bmatrix} 1 & -\frac{G_{12}(s)}{G_{11}(s)} \\ -\frac{G_{21}(s)}{G_{22}(s)} & 1 \end{bmatrix}$$

If $G_{11}(s)$ and $G_{22}(s)$ are second-order system or any other higher order system, to obtain a fixed structure of PI controller, they can be approximated by the first order plus dead time (FOPDT) model using the frequency response [34]. The FOPDT model for the each subsystem is obtained as

$$(27) \quad G_{ii}(s) = \frac{K_{ii}e^{-t_{di}s}}{T_{ii}s + 1}$$

However, for the FOPDT model as expressed in Eq.(27), the dead time is not considered for designing the feedback controller and the forward controller but it is used for the feedforward controller design to improve performance of reference tracking for reducing the transient response time. Thus, the transfer function in Eq. (27) is estimated as the first-order system as follows

$$(28) \quad G_{ii}(s) = \frac{B_p(s)}{A_p(s)} = \frac{b_{p0}}{a_{p1}s + a_{p0}} = \frac{K_{ii}}{T_{ii}s + 1}$$

where $B_p(s)$ and $A_p(s)$ are numerator and denominator polynomials of $G_{ii}(s)$.

A PI controller structure is given by

$$(29) \quad G_{ci}(s) = \frac{B_{ci}(s)}{A_{ci}(s)} = \frac{b_{c1}s + b_{c0}}{s} = K_{ci} \left(1 + \frac{1}{t_i s}\right) = \frac{K_{ci}s + K_{ci}/t_i}{s}$$

Substitute Eqs. (28) and (29) in Eq. (2) to obtain

$$(30) \quad P(s) = T_{ii}s^2 + (1 + K_{ii}K_{ci})s + K_{ii}K_{ci}/t_i$$

As the settling time t_s is defined to get the equivalent time constant τ from Eq. (6), a target characteristic polynomial is then

$$(31) \quad P_{target}(s) = a_0 \left[\frac{\tau^2}{\gamma_1} s^2 + \tau s + 1 \right]$$

By rearranging Eqs. (30) and (31), these are PI controller parameters tuned as follows

$$(32) \quad K_{ci} = \frac{1}{K_{ii}} \left(\frac{\gamma_1 T_{ii}}{\tau} - 1 \right)$$

$$(33) \quad t_i = \tau \left(1 - \frac{\tau}{\gamma_1 T_{ii}} \right)$$

For the forward controller design, $B_f(s)$ is equal to b_{c0} in Eq. (29) in case of the reference signal of unit step input that is $B_f(s) = b_{c0}$ and the transfer function of forward controller is then

$$(34) \quad G_{fi}(s) = \frac{B_f(s)}{B_c(s)} = \frac{b_{c0}}{b_{c1}s + b_{c0}} = \frac{K_{ci}/t_i}{K_{ci}s + K_{ci}/t_i}$$

The feedforward controllers added in TITO system with inverted decouplers as shown in Fig. 5 are considered as the lead compensator with transfer function structure as follows [24]

$$(35) \quad G_{ffi}(s) = \frac{B_{ff}(s)}{A_{ff}(s)} = \frac{\alpha_i T_{di}s + \beta_i}{T_{di}s + 1}$$

The values of α_i and β_i must be appropriately chosen and T_{di} is the derivative time obtained by the reaction curve of system [35]. Substituting $A_c(s)$ and $B_f(s)$ from Eqs. (29) and (34), respectively, and $B_{ff}(s)$ and $A_{ff}(s)$ from Eq.(35) into Eq. (17) and rearranging in the second-order transfer function yields

$$(36) \quad F(s) = B_f(s)A_{ff}(s) + B_{ff}(s)A_c(s) = m_2s^2 + m_1s + m_0 \\ = \alpha_i T_{di}s^2 + \left(\beta_i + \frac{T_{di}K_{ci}}{t_i} \right) s + \frac{K_{ci}}{t_i}$$

The tuning factor ν is then specified to regulate the response time of control system by using the values of γ_1 and τ as same the PI controller using CDM in the previous design. Therefore, the numerator polynomial for closed-loop control is then

$$(37) \quad F_{target}(s) = b_0 \left[\frac{(\nu\tau)^2}{\gamma_1} s^2 + \nu\tau s + 1 \right]$$

and by rearranging Eqs. (36) and (37), the feedforward controller parameters are then calculated by

$$(38) \quad \beta_i = \frac{K_{ci}}{t_i} (\nu\tau - T_{di})$$

$$(39) \quad \alpha_i = \frac{(\nu\tau)^2 K_{ci}}{\gamma_1 T_{di} t_i}$$

Simulation Results and Discussion

A well-known TITO system of the Wood and Berry distillation column process [19] is used as a case study for the decentralized PI controller design using CDM and CDM with FFC based on inverted decoupling. This transfer function matrix of process can be written as

$$(40) \quad G(s) = \begin{bmatrix} \frac{12.8e^{-s}}{16.7s + 1} & \frac{-18.9e^{-3s}}{21s + 1} \\ \frac{6.6e^{-7s}}{10.9s + 1} & \frac{-19.4e^{-3s}}{14.4s + 1} \end{bmatrix}$$

The inverted decoupler determined using Eq. (26) is

$$(41) \quad D(s) = \begin{bmatrix} 1 & \frac{1.477(16.7s + 1)e^{-2s}}{(21s + 1)} \\ \frac{0.34(14.4s + 1)e^{-4s}}{(10.9s + 1)} & 1 \end{bmatrix}$$

Therefore, from Eq. (25) the product of transfer function matrix of TITO process is then

$$(42) \quad T(s) = \begin{bmatrix} G_{11}(s) & 0 \\ 0 & G_{22}(s) \end{bmatrix} = \begin{bmatrix} \frac{12.8e^{-s}}{16.7s + 1} & 0 \\ 0 & \frac{-19.4e^{-3s}}{14.4s + 1} \end{bmatrix}$$

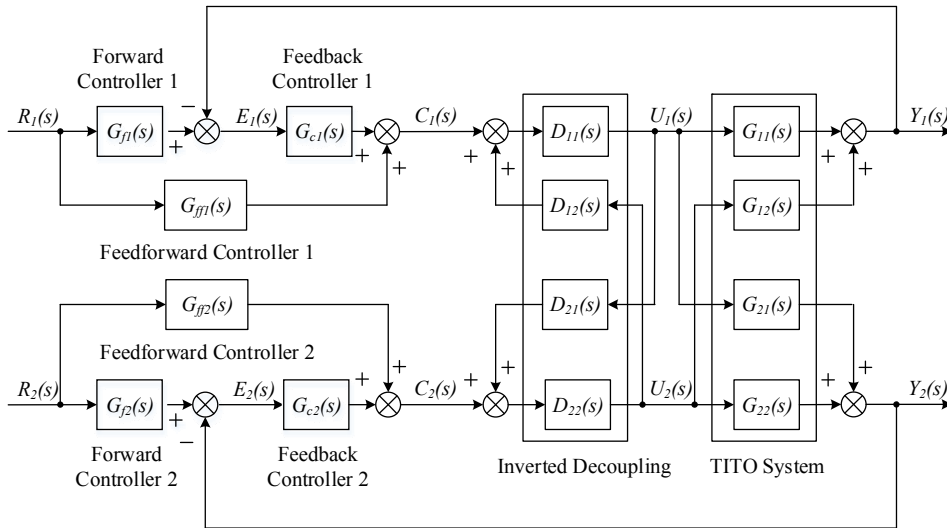


Fig.5. Block diagram of TITO system with inverted decoupler incorporating feedforward controller

The controller parameters of TITO process based on the inverted decoupling is determined when the FOPDT models of both subsystems of $G_{11}(s)$ for loop-1 ($y_1 - r_1$) and $G_{22}(s)$ for loop-2 ($y_2 - r_2$) are obtained. Then, the 2-DOF control strategy is applied to design the PI controller parameters by using CDM. The condition values of the equivalent time constants, τ , are 8 estimated by t_s of 24 min for loop-1 and 16 estimated by t_s of 48 min for loop-2, and the stability index, γ_i , of both loops is fixed at 3. Hence, the transfer function matrix of feedback controllers and forward controllers of loop-1 and loop-2 using CDM can be respectively written as

$$(43) \quad G_c(s) = \begin{bmatrix} \frac{0.4111s + 0.0612}{s} & 0 \\ 0 & \frac{-0.0876s - 0.0087}{s} \end{bmatrix}$$

$$(44) \quad G_f(s) = \begin{bmatrix} \frac{0.0612}{0.4111s + 0.0612} & 0 \\ 0 & \frac{0.0087}{0.0876s + 0.0087} \end{bmatrix}$$

By using CDM, it can be summarized that the PI controller parameters are $K_{p1} = 0.4111$, $K_{i1} = 0.0612$ and $t_{i1} = 6.7226$ min for loop-1 and $K_{p2} = -0.0876$, $K_{i2} = 0.0087$ and $t_{i2} = 10.0689$ min for loop-2. In the case of adding FFC in the TITO system with inverted decouplers, the transfer function matrix of FFC relating to Eq. (35) for loop-1 and loop-2 can be given by

$$(45) \quad G_{ff}(s) = \begin{bmatrix} \frac{\alpha_1 T_{d1}s + \beta_1}{T_{d1}s + 1} & 0 \\ 0 & \frac{\alpha_2 T_{d2}s + \beta_2}{T_{d2}s + 1} \end{bmatrix}$$

Table 1. The FFC controller parameters at different tuning factors

Tuning factor (ν)	Loop-1			Loop-2		
	α_1	β_1	T_{d1}	α_2	β_2	T_{d2}
0.3	0.2348	0.1162	0.5	-0.0445	-0.0287	1.5
0.5	0.6523	0.2141	0.5	-0.1237	-0.0565	1.5
0.7	1.2786	0.3119	0.5	-0.2425	-0.0844	1.5

The values of α_1 , β_1 and T_{d1} designed for loop-1 and α_2 , β_2 and T_{d2} designed for loop-2 depend on the tuning factor, ν , varied between 0.3 and 0.7 as shown in Table 1.

In this simulation of the Wood and Berry distillation column process for the PI controller system designed by using CDM and CDM with FFC at different tuning factors of 0.3, 0.5 and 0.7, a unit step change in set-point of loop-1 (y_1) and of loop-2 (y_2) is applied at time $t = 0$ min and at time $t = 150$ min, respectively. For loop-1, the output responses and the control signals are shown in Figs. 6 and 7, respectively. For loop-2, the output responses and the control signals are shown in Figs. 8 and 9, respectively. The comparison of controller performance in term of the settling time, t_s , the percent overshoot, P.O., and the maximum change of control signal, Δu_{max} , for the control design using CDM and CDM with FFC is given in Table 2.

Table 2. Settling time, percent overshoot and maximum change of control signal of loop-1 and loop-2

Controllers	Loop-1			Loop-2		
	t_s (min)	P.O.(%)	Δu_{max}	t_s (min)	P.O.(%)	Δu_{max}
CDM PI	19.25	0	0.2132	34.20	0.5	0.1134
CDM PI with FFC at $\nu = 0.3$	16.79	0.13	0.2510	30.15	0.5	0.1155
CDM PI with FFC at $\nu = 0.5$	15.17	0.20	0.6524	26.10	0.4	0.1274
CDM PI with FFC at $\nu = 0.7$	14.30	0.30	1.2787	17.85	0.2	0.2434

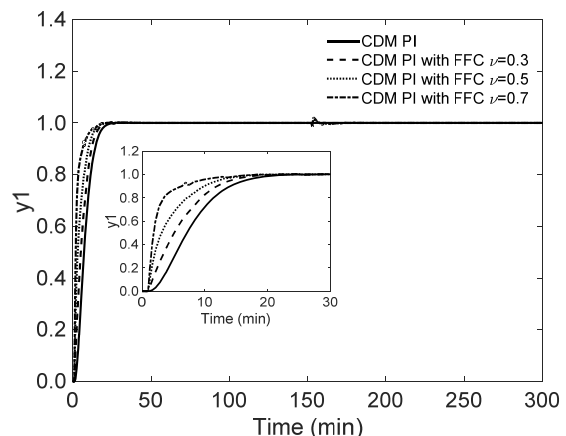


Fig.6. Unit step response of the loop-1 ($y_1 - r_1$)

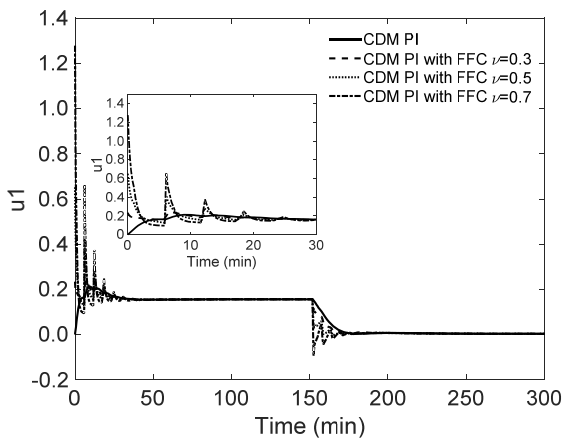


Fig. 7. Control signal response of the loop-1 (u_1)

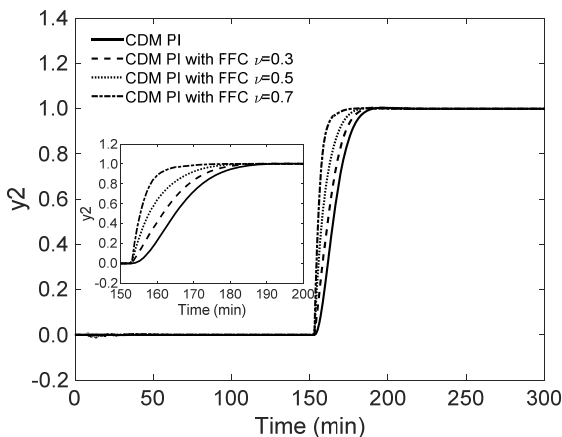


Fig. 8. Unit step response of the loop-2 (y_2-r_2)

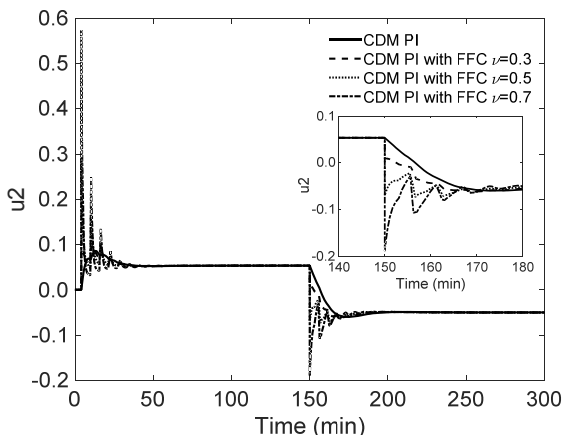


Fig. 9. Control signal response of the loop-2 (u_2)

The results presented that the output responses of both loops provide good performance for controlling the TITO process variables. When the method of PI controller design using CDM is compared with CDM combining FFC, the CDM shows an appropriate settling time in range of specified values of 24 min for loop-1 and 48 min for loop-2 as shown in Table 2 and very small percent overshoot can be neglected for both loops whereas the faster settling time can be achieved while the FFC is added to the control system. An increase of tuning factor decreases settling time but increases the maximum change of control signal.

The control performance of the proposed controller design using CDM with FFC at a tuning factor of 0.3, which obtains very flattened control action, is compared with other controller designs presented by Maghade and Patre ($G_c(s)MP$) [4] and Tavakoli ($G_c(s)Tavakoli$) [6] using the

decoupling from Eq. (41). The parameters of controllers of $G_c(s)MP$ and $G_c(s)Tavakoli$ are as follows

$$(46) \quad G_c(s)MP = \begin{bmatrix} \frac{0.9733 + \frac{0.0881}{s} + 2.6887s}{(5.5252s+1)} & 0 \\ 0 & \frac{-0.3134 - \frac{0.0304}{s} - 0.8070s}{(5.1499s+1)} \end{bmatrix}$$

$$(47) \quad G_c(s)Tavakoli = \begin{bmatrix} 0.410 + \frac{0.074}{s} & 0 \\ 0 & -0.120 - \frac{0.024}{s} \end{bmatrix}$$

The controller ($G_c(s)MP$) is introduced in literature with desired Gain Margin (GM) = 3, and Phase Margin (PM) = 60° , while the controller ($G_c(s)Tavakoli$) is considered when $GM \geq 3$ and $PM \geq 60^\circ$ as the robustness constraints, then the optimal PI tuning parameters are calculated.

For simulation results, when the different methods of control system design for the Wood and Berry distillation process are compared, a unit step change is set at the set-point inputs for loop-1 at time $t = 0$ min and for loop-2 at time $t = 150$ min and the disturbance inputs at y_1 for time $t = 250$ min and at y_2 for time $t = 400$ min. The comparisons between different control design methods of the output response and the control signal of loop-1 are illustrated in Figs. 10 and 11, respectively. Additionally, the comparisons between different control design methods of the output response and the control signal of loop-2 are demonstrated in Figs. 12 and 13, respectively. In case of a set-point change, the output responses for proposed controller of both loops present good performance with speedier settling time; lower percent overshoot of response; and smaller the maximum change of control signal than controller design introduced by Maghade and Patre [4] and Tavakoli [6] as shown in Table 3.

Table 3. Output response and controller response parameters of proposed controller and other controllers for unit step change

Controllers	Loop-1			Loop-2		
	t_s (min)	P.O.(%)	Δu_{max}	t_s (min)	P.O.(%)	Δu_{max}
Proposed	16.79	0.13	0.2510	30.15	0.5	0.1155
Maghade and Patre	34.00	21.00	0.5620	53.50	41.2	0.2474
Tavakoli	27.00	17.80	0.4740	41.00	20.8	0.1934

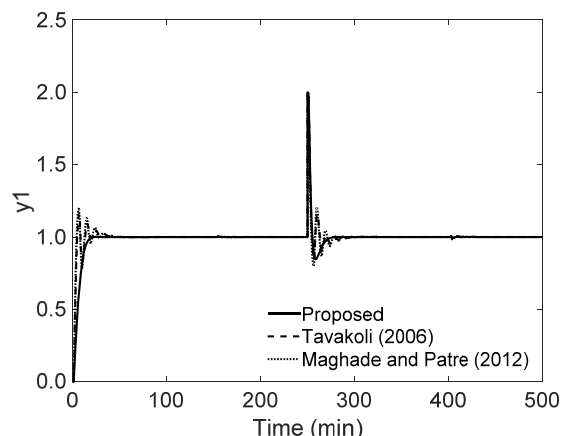


Fig. 10. Comparison of unit step response of the loop-1 (y_1-r_1)

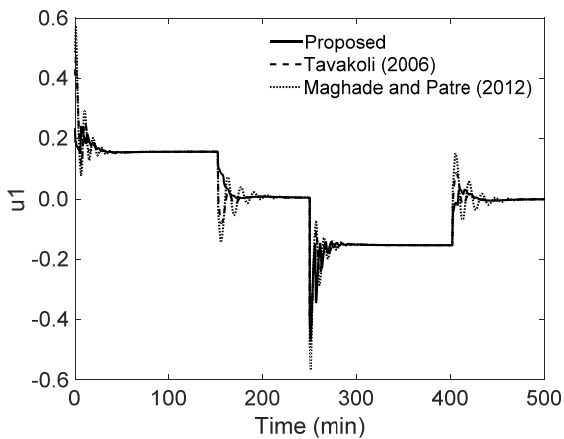


Fig. 11. Comparison of control signal response of the loop-1 (u_1)

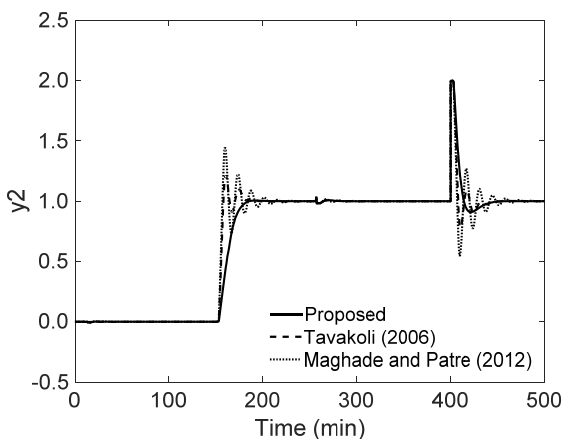


Fig. 12. Comparison of unit step response of the loop-2 (y_2-r_2)

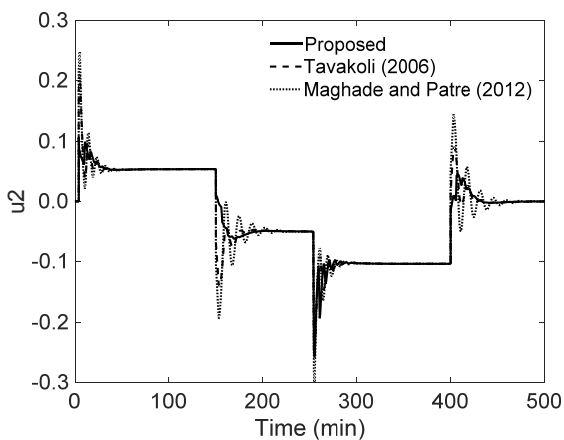


Fig. 13. Comparison of control signal response of the loop-2 (u_2)

In case of disturbance inputs, the output responses for the proposed controllers of both loops provide the competitive performance with the desired transient responses and smaller the maximum change of control signal than controllers design introduced by Maghade and Patre [4] and Tavakoli [6] as shown in Table 4.

Table 4. Output response and controller response parameters of proposed controller and other controllers for disturbance input

Controllers	Loop-1		Loop-2	
	t_s (min)	Δu_{max}	t_s (min)	Δu_{max}
Proposed	20.3	0.4682	38.92	0.1347
Maghade and Patre	26.0	0.5690	30.07	0.1934
Tavakoli	18.0	0.4809	59.44	0.2477

Conclusion

A decentralized PI controller using two design methods of CDM and CDM with FFC for a TITO process combined the inverted decoupling is proposed. By using the inverted decoupling, the TITO process is reduced loop interactions to be SISO system as function of FOPDT model. The parameters of PI controllers determined by using CDM with FFC give better performance than that using CDM. The CDM incorporating FFC obtains the fast transient response with tiny peak overshoot although the maximum change of control signal obviously increases. In addition, the proposed controllers give smooth changes during sudden unit step changes and external disturbance inputs.

Authors: Mr. Chananchai Wutthithanyawat, Pathumwan Institute of Technology, 833 Rama I road, Pathumwan, Bangkok 10330, Thailand, E-mail: chananchai.wut@gmail.com; Assoc. Prof. Dr. Santi Wangnipparnto, Pathumwan Institute of Technology, 833 Rama I road, Pathumwan, Bangkok 10330, Thailand, E-mail: nipparnto@gmail.com.

REFERENCES

- [1] Hajare V.D., Patre B.M., Decentralized PID controller for TITO systems using characteristic ratio assignment with an experimental application, *ISA Trans.*, 59 (2015), 385-397
- [2] Bhat V.S., Thirunavukkarasu I., Shanmuga P.S., Design and Implementation of Decentralized Pi Controller for Pilot Plant Binary Distillation Column, *Int. J. Chemtech Res.*, 10 (2017), 284-294
- [3] Nandonga J., Zang Z., Multi-loop design of multi-scale controllers for multivariable processes, *J. Process Control*, 24 (2014), 600-612
- [4] Maghadea D.K., Patre B.M., Decentralized PI/PID controllers based on gain and phase margin specifications for TITO processes, *ISA Trans.*, 51 (2012), 550-558
- [5] Dong J., Sun L., Li D., Lee K.Y., Wu Z., Inverted Decoupling based Active Disturbance Rejection Control for Multivariable Systems, *Proceeding of IEEE 54th Annual Conference on Decision and Control (CDC)*, (2015), 7353-7358
- [6] Tavakoli S., Griffin I., Fleming P.J., Tuning of decentralised PI (PID) controllers for TITO processes, *Control Eng. Pract.*, 14 (2006), 1069-1080.
- [7] Jin Q., Wang Q., Liu L., Design of decentralized proportional-integral-derivative controller based on decoupler matrix for two-input/two output process with active disturbance rejection structure, *Adv. Mech. Eng.*, 8 (2016), 1-18
- [8] Wade H.L., Inverted decoupling: a neglected technique, *ISA Trans.*, 36 (1997), 3-10
- [9] Gagnon E., Pomerleau A., Desbiens A., Simplified, ideal or inverted decoupling?, *ISA Trans.*, 37 (1998), 265-276
- [10] Garrido J., Vázquez F., Morilla F., Hägglund T., Practical advantages of inverted decoupling, *Proceeding of the Institution of Mechanical Engineers, Part I: Journal of Systems and Control Engineering*, 225 (2011), 977-992
- [11] Kumar V.P., A Comparative Study on Decoupling Methods for Time-Delay Systems [master thesis], Department of Electrical Engineering, National Institute of Technology Rourkela, (2015)
- [12] Chen P., Zhang W., Improvement on an inverted decoupling technique for a class of stable linear multivariable processes, *ISA Trans.*, 46 (2007), 199-210
- [13] Mekki I.E.K., A Comparative Study of Control Design Methods PI Applied to a Distillation Column, *International Journal of Science and Advanced Technology*, 4 (2014), 6-10
- [14] Vrančić D., Design of MIMO Controllers with inverted decoupling, *Proceeding of 2011 8th Asian Control Conference (ASCC)*, (2011), 1153-1158
- [15] Garrido J., Vázquez F., Morilla F., Smith Predictor with Inverted Decoupling for stable TITO Processes with Time Delays, *Proceeding of 2014 IEEE Emerging Technology and Factory Automation (ETFA)*, (2014), 1-8
- [16] Hariz M.B., Bouani F., Design of controllers for decoupled TITO systems using different decoupling techniques, *Proceeding of 2015 IEEE 20th International Conference on Methods and Models in Automation and Robotics (MMAR)*, (2015), 1116-1121

- [17] Wutthithanyawat C. and Wangnipparnto S., Design of decentralized PID controller with the root locus method based on inverted decoupling for a TITO system, *Journal of Thai Interdisciplinary Research*, 13 (2018), 18-24
- [18] Wutthithanyawat C. and Wangnipparnto S., Design of Decentralized PID Controller with Coefficient Diagram Method based on Inverted Decoupling for TITO System, *Proceeding of IECON 2018, Krabi, Thailand*, (2018)
- [19] Wood R.K., Berry M.W., Terminal composition control of a binary distillation column, *Chem. Eng. Sci.*, 28 (1973), 1707-1717
- [20] Rinu Raj R.R., Vijay Anand L.D., Design and Implementation of a CDM-PI Controller for a Spherical Tank Level System, *International Journal on Theoretical and Applied Research in Mechanical Engineering*, 2 (2013), 49-52
- [21] Vu T.N.L., Lee M., Multi-loop PI controller design based on the direct synthesis for interacting multi-time delay processes, *ISA Trans.*, 49 (2010), 79-86
- [22] Wang Q.G., Huang B., Guo X., Auto-tuning of TITO decoupling controllers from step tests, *ISA Trans.*, 39 (2000), 407-418
- [23] Sirsat M.P., Parvat B.J., Kadu C.B., Design Of Decentralized PI Controller For Two-Input, Two-Output Processes, *Proceeding of 2015 International Conference on Energy Systems and Applications (ICESA 2015)*, Pune, India, (2015), 451-455
- [24] Kumpanya D., Benjanarasuth T., Ngamwiwit J., Komine N., PI controller design with feedforward by CDM for level processes, *Proceeding of 2000 TENCON Intelligent Systems and Technologies for the New Millennium (Cat. No.00CH37119)*, Kuala Lumpur, Malaysia, (2000), II65-II69
- [25] Benjanarasuth T., Kumpanya D., Komine N., Ngamwiwit J., FFC Incorporating PI Controller Designed by CDM for Temperature Control Systems, *Proceeding of IEEE ICIT'02, Bangkok, Thailand*, (2002), 540-544
- [26] Kumpanya D., Benjanarasuth T., Ngamwiwit J., Komine N., FFC Designed for PI Flow Control System Designed by CDM, *Proceedings of the 2001 International Conference on Control, Automation and Systems, Jeju, Korea*, (2001), 1052-1055
- [27] Isarakorn D., Suksariwattanagul N., Benjanarasuth T., Ngamwiwit J., Komine N., Two-Degree-of-Freedom Controller Designed by Coefficient Diagram Method, *Proceeding of the 2004 International Conference on Control, Automation and Systems, Bangkok, Thailand*, (2004), 262-267
- [28] Suksri T., Tunyasrirut S., Two-DOF Controller Designed by CDM Incorporating FFC for a Smith Predictor Scheme, *Proceeding of ICROS-SICE International Joint Conference 2009, Fukuoka International Congress Center, Japan*, (2009), 2510-2515
- [29] Khuakoonratt N., Benjanarasuth T., Ngamwiwit J., Komine N., I-PDA Incorporating FFC Control System Designed by CDM, *Proceeding of SICE Annual Conference in Fukui, Fukui University, Japan*, (2003), 2250-2254
- [30] Manabe S., Coefficient Diagram Method, *Proceeding of the 14th IFAC Symposium on Automatic Control in Aerospace*, (1998), 199-210
- [31] Manabe S., Importance of Coefficient Diagram in Polynomial Method, *Proceeding of the 42nd IEEE Conference on Decision and Control*, (2003), 3489-3494
- [32] Isarakorn D., Panaudomsup S., Benjanarasuth T., Ngamwiwit J., Komine N., Application of CDM to PDF Controller for Motion Control System, *Proceeding of the 4th Asian Control Conference*, (2002), 1173-1177
- [33] Li Z., Chen Y.Q., Ideal, Simplified and Inverted Decoupling of Fractional Order TITO Processes, *IFAC Proceedings Volumes*, 47 (2014), 2897-2902
- [34] Wang Q.G., Lee T.H., Lin C., *Relay feedback: analysis, identification and control*, 2nd edition, London, Springer, (2003)
- [35] Ziegler J.G., Nichols N.B., Optimum Settings for Automatic Controllers, *Transactions of the A.S.M.E.*, (1942), 759-765